A novel optical flow method based on a second-order non-linear differential equation

R. G. González-Acuña

Huawei Technologies, Camera Lab, Korkeakoulunkatu 7, 33720 Tampere, Finland.

Received 13 August 2024; accepted 15 October 2024

A novel optical flow algorithm based on a second-order nonlinear differential equation is presented. This equation expresses the difference between two sequential images, and from its solution, the optical flow information between the images can be extracted. The new algorithm is compared with standard optical flow algorithms, as well as some of their recent generalizations. The comparisons are conducted using common tests applied in particle image velocimetry. The results show that the new algorithm outperforms classical algorithms in these particular tests

Keywords: Optical flow; second-order; algorithm.

DOI: https://doi.org/10.31349/RevMexFis.71.021301

1. Introduction

Optical flow refers to the pattern of apparent movement of objects, surfaces, and edges in a scene, caused by the relative motion between an observer and the scene [1]. The main applications of optical flow include detection, speed determination [2,3], deformation measurements [4,5], displacement measurement [6], particle velocimetry [7], and fluid motion analysis [8,9], among others.

Optical flow can be computed from a sequence of images. Most optical flow algorithms work with two consecutive images of the same scene [10,11]. The most commonly used optical flow algorithms are the Lucas-Kanade algorithm and the Horn-Schunck method [10-13]. The basic assumptions of the Lucas-Kanade algorithm are that the flow is essentially constant within a local neighborhood of the pixel under consideration, and that it solves the optical flow equations for all pixels in that neighborhood. The algorithm divides the image into small windows/neighborhoods and computes the velocity of a particular neighborhood using a least-squares method [10,14].

The Horn-Schunck method, on the other hand, is an optical flow algorithm that estimates the velocity globally instead of using local windows/neighborhoods [11]. Both algorithms have several generalizations and extensions, including those incorporating artificial intelligence [13], fractional calculus [15-17], pyramid implementations [9], fuzzy logic [18], and more. Notably, applying fractional calculus to optical flow has improved performance under certain conditions [15].

Here, a novel optical flow algorithm based on a second-order nonlinear differential equation is presented. The mentioned differential equation is solved using a least-squares method in an iterative process. This manuscript is organized as follows: In Sec. 2, the mathematical derivation of the second-order nonlinear differential equation and its solution using the least-squares method is presented. In Sec. 3, the novel algorithm is tested against the Kanade algorithm [10], the Horn-Schunck method [11], and their fractional versions. The test follows a standard procedure in optical flow. Finally, in Sec. 4, the conclusions are provided.

2. Mathematical model

The goal of the algorithm presented in this manuscript is to determine the optical flow between two consecutive images. Let u and v represent the pixel displacements between the images in the x and y directions, respectively. Consequently, if the first image $I_1(x, y)$ is displaced to $I_1(x + u, y + v)$, it should resemble the second image $I_2(x, y)$. The objective of the algorithm is to find u and v such that the differences between $I_1(x+u, y+v)$ and $I_2(x, y)$ are minimized. In the following derivation, the dependence on independent variables is omitted to simplify the notation. Thus, $I_1(x, y) = I_1$ and $I_2(x, y) = I_2$.

From the derivation of the Lucas-Kanade algorithm, we can consider the total differential of the first image $I_1(x, y)$ to be equal to the negative derivative of the first image concerning time t,

$$\frac{\partial I_1}{\partial x}u + \frac{\partial I_1}{\partial y}v = -\frac{\partial I_1}{\partial t}, \tag{1}$$

derivating Eq. (1) respect to x and multiplied by u,

$$u\frac{\partial^2 I_1}{\partial x \partial t} = -u^2\frac{\partial^2 I_1}{\partial x^2} - uv\frac{\partial^2 I_1}{\partial x \partial y}. \tag{2}$$

Independently, derivating Eq. (1) it respect to y and multiplied by v,

$$v\frac{\partial^2 I_1}{\partial y \partial t} = -v^2\frac{\partial^2 I_1}{\partial y^2} - uv\frac{\partial^2 I_1}{\partial x \partial y}. \tag{3}$$

Now, on the other hand, we take the first image evaluated with the displacements u and v in horizontal and vertical directions respectively and then we expand it in the Taylor series, taking also the first non-linear terms,

$$I_1(x+u,y+v) = I_1 + u\frac{\partial I_1}{\partial x} + v\frac{\partial I_1}{\partial y} + \frac{1}{2}\left(u^2\frac{\partial^2 I_1}{\partial x^2} + v^2\frac{\partial^2 I_1}{\partial y^2} + 2uv\frac{\partial I_1}{\partial x}\frac{\partial I_1}{\partial y}\right). \tag{4}$$

Then, if we take equation Eq. (2) and Eq. (3) and substitute them in equation Eq. (4) we have,

$$I_1(x+u,y+v) = I_1 + u\frac{\partial I_1}{\partial x} + v\frac{\partial I_1}{\partial y} - \frac{1}{2}\left(u\frac{\partial^2 I_1}{\partial x\partial t} + v\frac{\partial^2 I_1}{\partial y\partial t}\right). \tag{5}$$

Observe that Eq. (5) does not have non-linear terms, but it has not lost its information. Therefore, the least squares can be used to compute the error estimation of the difference of $I_1(x+u,y+v) - I_2(x,y)$,

$$E = \sum_i\sum_j \left[I_1 + u\frac{\partial I_1}{\partial x} + v\frac{\partial I_1}{\partial y} - \frac{1}{2}\left(u\frac{\partial^2 I_1}{\partial x\partial t} + v\frac{\partial^2 I_1}{\partial y\partial t}\right) - I_2\right]^2, \tag{6}$$

where $\sum_i$ and $\sum_j$ are the sums over the windows/neighborhoods. If we want to minimize the error, we need to derivative Eq. (6) concerning u and v and equal to zero. Thus, in u,

$$0 = \sum_i\sum_j \left[I_1 + u\frac{\partial I_1}{\partial x} + v\frac{\partial I_1}{\partial y} - \frac{1}{2}\left(u\frac{\partial^2 I_1}{\partial x\partial t} + v\frac{\partial^2 I_1}{\partial y\partial t}\right) - I_2\right]\left(\frac{\partial I_1}{\partial x} - \frac{1}{2}\frac{\partial^2 I_1}{\partial x\partial t}\right), \tag{7}$$

in v,

$$0 = \sum_i\sum_j \left[I_1 + u\frac{\partial I_1}{\partial x} + v\frac{\partial I_1}{\partial y} - \frac{1}{2}\left(u\frac{\partial^2 I_1}{\partial x\partial t} + v\frac{\partial^2 I_1}{\partial y\partial t}\right) - I_2\right]\left(\frac{\partial I_1}{\partial y} - \frac{1}{2}\frac{\partial^2 I_1}{\partial y\partial t}\right). \tag{8}$$

Expanding and reordering the terms, in Eq. (7),

$$\sum_i\sum_j (I_2 - I_1)\left(\frac{\partial I_1}{\partial x} - \frac{1}{2}\frac{\partial^2 I_1}{\partial x\partial t}\right) = \sum_i\sum_j u\left(\frac{\partial I_1}{\partial x} - \frac{1}{2}\frac{\partial^2 I_1}{\partial x\partial t}\right)^2 + \sum_i\sum_j v\left(\frac{\partial I_1}{\partial y} - \frac{1}{2}\frac{\partial^2 I_1}{\partial y\partial t}\right)\left(\frac{\partial I_1}{\partial x} - \frac{1}{2}\frac{\partial^2 I_1}{\partial x\partial t}\right), \tag{9}$$

and expanding and reordering the terms, but now in Eq. (8)

$$\sum_i\sum_j (I_2 - I_1)\left(\frac{\partial I_1}{\partial y} - \frac{1}{2}\frac{\partial^2 I_1}{\partial y\partial t}\right) = \sum_i\sum_j u\left(\frac{\partial I_1}{\partial x} - \frac{1}{2}\frac{\partial^2 I_1}{\partial x\partial t}\right)\left(\frac{\partial I_1}{\partial y} - \frac{1}{2}\frac{\partial^2 I_1}{\partial y\partial t}\right) + \sum_i\sum_j v\left(\frac{\partial I_1}{\partial y} - \frac{1}{2}\frac{\partial^2 I_1}{\partial y\partial t}\right)^2. \tag{10}$$

The above equations can be expressed in a matrix form,

$$\begin{bmatrix} \sum_i\sum_j \left(\frac{\partial I_1}{\partial x} - \frac{1}{2}\frac{\partial^2 I_1}{\partial x\partial t}\right)^2 & \sum_i\sum_j \left(\frac{\partial I_1}{\partial y} - \frac{1}{2}\frac{\partial^2 I_1}{\partial y\partial t}\right)\left(\frac{\partial I_1}{\partial x} - \frac{1}{2}\frac{\partial^2 I_1}{\partial x\partial t}\right) \\ \sum_i\sum_j \left(\frac{\partial I_1}{\partial x} - \frac{1}{2}\frac{\partial^2 I_1}{\partial x\partial t}\right)\left(\frac{\partial I_1}{\partial y} - \frac{1}{2}\frac{\partial^2 I_1}{\partial y\partial t}\right) & \sum_i\sum_j \left(\frac{\partial I_1}{\partial y} - \frac{1}{2}\frac{\partial^2 I_1}{\partial y\partial t}\right)^2 \end{bmatrix} \begin{bmatrix} u \\ v \end{bmatrix} = \begin{bmatrix} \sum_i\sum_j (I_2 - I_1)\left(\frac{\partial I_1}{\partial x} - \frac{1}{2}\frac{\partial^2 I_1}{\partial x\partial t}\right) \\ \sum_i\sum_j (I_2 - I_1)\left(\frac{\partial I_1}{\partial y} - \frac{1}{2}\frac{\partial^2 I_1}{\partial y\partial t}\right) \end{bmatrix}. \tag{11}$$

The solution of Eq. (11) is Eq. (12),

$$\begin{bmatrix} u \\ v \end{bmatrix} = \begin{bmatrix} \sum_i\sum_j \left(\frac{\partial I_1}{\partial x} - \frac{1}{2}\frac{\partial^2 I_1}{\partial x\partial t}\right)^2 & \sum_i\sum_j \left(\frac{\partial I_1}{\partial y} - \frac{1}{2}\frac{\partial^2 I_1}{\partial y\partial t}\right)\left(\frac{\partial I_1}{\partial x} - \frac{1}{2}\frac{\partial^2 I_1}{\partial x\partial t}\right) \\ \sum_i\sum_j \left(\frac{\partial I_1}{\partial x} - \frac{1}{2}\frac{\partial^2 I_1}{\partial x\partial t}\right)\left(\frac{\partial I_1}{\partial y} - \frac{1}{2}\frac{\partial^2 I_1}{\partial y\partial t}\right) & \sum_i\sum_j \left(\frac{\partial I_1}{\partial y} - \frac{1}{2}\frac{\partial^2 I_1}{\partial y\partial t}\right)^2 \end{bmatrix}^{-1} \times \begin{bmatrix} \sum_i\sum_j (I_2 - I_1)\left(\frac{\partial I_1}{\partial x} - \frac{1}{2}\frac{\partial^2 I_1}{\partial x\partial t}\right) \\ \sum_i\sum_j (I_2 - I_1)\left(\frac{\partial I_1}{\partial y} - \frac{1}{2}\frac{\partial^2 I_1}{\partial y\partial t}\right) \end{bmatrix}. \tag{12}$$

Equation (12) is the most important equation in the presented manuscript. It describes how the displacements u and v are such that the error estimation of the difference of $I_1(x+u, y+v) - I_2(x, y)$ is minimized. The computation of Eq. (12) can be presented in a loop to improve the algorithm's performance.

The second derivative of I_1 with respect to x and time t is the numerical difference between I_1-I_2, derivated respect to x.

3. Experimental results and performance

Equation (12) will be tested using a common optical flow scenario derived from particle image velocimetry (PIV). PIV is a non-intrusive optical measurement technique used to study fluid flow patterns and velocities [7,19,20]. The test involves generating particles with Gaussian profiles at random positions along the rows and columns of an image. The complete simulation consists of two images: one showing the initial positions of the particles and another showing the particles after a known displacement [19].

The numerical analysis considers the following data selection: The image size is 250×250 pixels, with 6,000 particles in each image. The particle diameters range from 1 to 4 pixels. The selected displacement is a curl displacement,

$$u = A(v - x_c) + \text{noise}, \quad v = -A(u - y_c) + \text{noise}, \quad (13)$$

where A represents the amplitude of the displacement, typically set to $A = 1/25$. The noise in the displacement is random, ranging from -2 to +2 pixels. The center of the vortex for the curl displacement is located at $x_c = 117$ and $y_c = 158$. For the Lucas-Kanade algorithm, its fractional version, and the new algorithm, the scan window size was 10×10 pixels, and the algorithms ran for 7 iterations. Finally, the number of iterations for the Horn-Schunck method and its fractional version was set to 30.

To evaluate the mentioned methods, the percentage of relative error is computed in its components, [19]

$$E_u = \sqrt{\frac{\sum_{i=1}^{n}(u_g^i - u^i)^2}{n}}\frac{100}{\max(u_g)}, \quad (14)$$

$$E_v = \sqrt{\frac{\sum_{i=1}^{n}(v_g^i - v^i)^2}{n}}\frac{100}{\max(v_g)}, \quad (15)$$

where u_g and v_g given values of the displacements, n is the length of vector u and $\max(u)$ returns the maximum value of u.

The following tests will be performed under the assumption of ceteris paribus. Ceteris paribus is a term used to analyze the behavior of independent parameters while keeping other parameters constant. The parameters to be studied are the displacement size, the particle diameter D, and the number of particles m. All tests are conducted using a set of 50 PIV images.

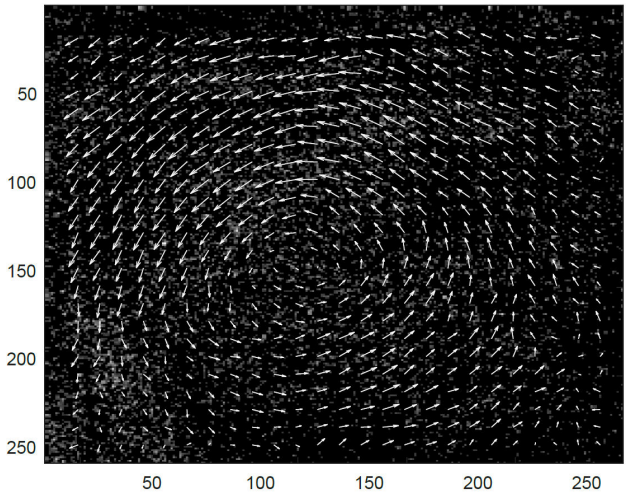

FIGURE 1. Optical flow detected by new algorithm for a circular displacement with amplitude $A = (1/75)$ pix.

Table I shows the results for varying the amplitude while keeping the other parameters constant. The performance of each algorithm is presented in a column of Table I in the following order: the new algorithm (NA), the Lucas-Kanade algorithm (LK) [10], the fractional Lucas-Kanade algorithm (FLK) [17], the Horn-Schunck method (HK) [11], and the Kumar-Horn-Schunck method (KHS) [15]. The experiment in Table I demonstrates the response of the algorithms as the amplitude A of the curl displacement increases. From the table, it is clear that the new algorithm outperforms the others for this particular task.

Tables II, III, and IV are presented in the same format as Table I, but they vary in terms of particle size, number of particles, and noise amplitude, respectively. In all tests, the new algorithm demonstrated superior performance. Figure 1 presents the analysis of the optical flow detected by the new algorithm for a circular displacement. Additionally, from the values in Tables I, II, and III, it can be observed that the fractional versions generally perform better than their original counterparts.

The method presented here differs from the Lucas-Kanade algorithm [10] and the Horn-Schunck method [11] because it is based on a second-order nonlinear differential equation rather than a first-order differential equation. This

TABLE I. Performance of NA, LK, FLK, HK, KHS, in terms of the relative error for 50 sets of PIV images, and for different values of the amplitude A.

A[pix]	NA (%)	LK(%)	FLK(%)	HS(%)	KHS(%)
1/125	21.05	25.28	24.82	38.19	30.21
1/100	12.98	17.05	19.98	35.92	34.75
1/75	21.01	26.24	28.47	49.96	46.06
1/50	31.43	38.73	65.40	100.21	97.51
1/25	76	81	99	147	134

TABLE II. Performance of NA, LK, FLK, HK, KHS, in terms of the relative error for 50 sets of PIV images, and different values of the diameter range of the size of the particle pix.

D [pix]	NA (%)	LK(%)	FLK(%)	HS(%)	KHS(%)
(3,6)	22.89	32.34	32.21	52.99	48.96
(2,5)	21.06	27.97	29.92	50.67	47.68
(1,4)	21.01	26.24	28.47	49.9	46.06
(1,3)	22.08	27.21	26.99	51.46	44.89
(1,2)	16.08	37.98	29.26	55.98	51.78

TABLE III. Performance of NA, LK, FLK, HK, KHS, in terms of the relative error for 50 sets of PIV images, and for different number of particles.

m	NA (%)	LK(%)	FLK(%)	HS(%)	KHS(%)
8000	24.69	33.96	32.98	53.78	49.95
7000	21.05	31.11	26.87	48.74	44.07
6000	21.01	26.24	28.47	49.9	46.06
5000	23.61	30.19	33.36	56.64	47.97
4000	28.97	34.55	32.97	60.94	5.1.08

TABLE IV. Performance of NA, LK, FLK, HK, KHS, in terms of the relative error for 50 sets of PIV images, and for different noise applitude.

$\pm$ [pix]	NA (%)	LK(%)	FLK(%)	HS(%)	KHS(%)
0	21.11	25.22	24.67	41.86	30.75
1	21.51	28.10	25.25	42.90	33.54
2	23.17	29.98	29.08	44.41	32.91

method starts with two consecutive images of a scene, from which the differential equation is derived and solved using an iterative process with the least-squares algorithm. Like the Lucas-Kanade method, the algorithm is implemented in small windows or neighborhoods across the image. However, the proposed method considers more terms from the Taylor series than the Lucas-Kanade algorithm, which contributes to its superior performance. Although the new algorithm does not use fractional calculus, it still outperforms the fractional Lucas-Kanade algorithm because the fractional versions are based on fewer terms from the Taylor series.

The Lucas-Kanade algorithm is restricted to the first terms of the Taylor series and is therefore limited to the linear information they provide. While several generalizations of the Lucas-Kanade algorithm incorporate artificial intelligence and machine learning, we do not compare these generalizations in this manuscript. Our focus is on highlighting the additional terms from the Taylor series used by the new algorithm. A natural next step would be to integrate artificial intelligence into the new algorithm; however, this is beyond the scope of the paper due to the various approaches it could take and its open-ended nature.

4. Conclusion

In this manuscript, it was presented a novel algorithm to compute the optical flow between two consecutive images. The algorithm is based on a second-order non-linear differential equation, Eq. (6). The mentioned equation expresses the error difference between the consecutive images. The error is minimized with Eq. (12), which is the most important equation in the presented paper.

The new algorithm is compared with the Lucas-Kanade algorithm, the Horn-Schunck method, and their fractional versions using a standard test in particle-image velocimetry. The results show that the novel algorithm outperforms the other algorithms for this particular task. A natural next step in this research is to integrate the new algorithm with machine learning techniques.

Data availability

Data underlying the results presented in this paper are not publicly available at this time but may be obtained from the author upon reasonable request.

Funding

There is no funding award related to this research.

Disclosures

The author declares no conflicts of interest.

1. R. G. González-Acuña, H. A. Chaparro-Romo, and I. Melendez-Montoya, Optics and Artificial Vision (IOP Publishing, 2021).
2. D. Shukla and E. Patel, Speed determination of moving vehicles using Lucas-Kanade algorithm, *International Journal of Computer Applications Technology and Research* **2** (2013) 32, https://doi.org/10.7753/ijcatr0201.1007.
3. J. Guo *et al*., Vision-based measurement for rotational speed by improving Lucas-Kanade template tracking algorithm, *Applied optics* **55** (2016) 7186. https://doi.org/10.1364/AO.55.007186.
4. W. Tong, Formulation of Lucas-Kanade digital image correlation algorithms for non-contact deformation measurements: a review, *Strain* **49** (2013) 313. https://doi.org/10.1111/str.12039.
5. S. Shakya and S. Kumar, Characterising and predicting the movement of clouds using fractional-order optical flow, *IET*

Image Processing **13** (2019) 1375. https://doi.org/10.1049/iet-ipr.2018.6100.

6. T. Brox, C. Bregler, and J. Malik, Large displacement optical flow, In 2009 IEEE Conference on Computer Vision and Pattern Recognition (IEEE, 2009) pp. 41-48. https://doi.org/10.1109/CVPR.2009.5206697.

7. G. M. Quénot, J. Pakleza, and T. A. Kowalewski, Particle image velocimetry with optical flow, *Experiments in fluids* **25** (1998) 177. https://doi.org/10.1007/s003480050222.

8. T. Liu and L. Shen, Fluid flow and optical flow, *Journal of Fluid Mechanics* **614** (2008) 253. https://doi.org/10.1017/S0022112008003273.

9. Y. Liu *et al*., A new methodology for pixel-quantitative precipitation nowcasting using a pyramid Lucas Kanade optical flow approach, *Journal of Hydrology* **529** (2015) 354. https://doi.org/10.1016/j.jhydrol.2015.07.042.

10. B. Lucas, Generalized Image Matching by the Method of Differences, Ph.D. thesis, Carnegie-Mellon University (1984).

11. B. K. P. Horn and B. G. Schunck, Determining optical flow, *Artificial intelligence* **17** (1981) 185. https://doi.org/10.1016/0004-3702(81)90024-2.

12. A. M. G. Pinto *et al*., Revisiting lucas-kanade and hornschunck, *J. Comput. Eng. Inf* **1** (2013) 23. https://doi.org/10.5963/JCEI0102001.

13. S. Yao *et al*., Learning deep Lucas-Kanade Siamese network for visual tracking, *IEEE Transactions on Image Processing* **30** (2021) 4814, https://doi.org/10.1109/TIP.2021.3076272.

14. P. Docherty *et al*., Regressive cross-correlation of pressure signals in the region of stenosis: Insights from particle image velocimetry experimentation, *Biomedical Signal Processing and Control* **32** (2017) 143, https://doi.org/10.1016/j.bspc.2016.09.025.

15. P. Kumar, S. Kumar, and B. Raman, A fractional order variational model for the robust estimation of optical flow from image sequences, *Optik-International Journal for Light and Electron Optics* **127** (2016) 8710. https://doi.org/10.1016/j.ijleo.2016.05.118.

16. D. Chen *et al*., Fractional-order variational optical flow model for motion estimation, *Philosophical Transactions of the Royal Society A: Mathematical, Physical and Engineering Sciences* **371** (2013) 20120148. https://doi.org/10.1098/rsta.2012.0148.

17. R. G. González-Acuña, A. Dávila, and J. C. Gutiérrez-Vega, Optical flow of non-integer order in particle image velocimetry techniques, *Signal Processing* **155** (2019) 317. https://doi.org/10.1016/j.sigpro.2018.10.006.

18. Y. Lu *et al*., Optical flow detection based on enhanced fuzzy clustering with elastic grouping logic, In 4th International Symposium on Advanced Optical Manufacturing and Testing Technologies: *Optical Test and Measurement Technology and Equipment*, **7283** (2009) 578, https://doi.org/10.1117/12.828727.

19. M. Raffel *et al*., Particle image velocimetry: a practical guide (Springer, 2018). .

20. R. Yegavian *et al*., Lucas-Kanade fluid trajectories for timeresolved PIV, *Measurement science and Technology* **27** (2016) 084004. https://doi.org/10.1088/0957-0233/27/8/084004.

21. S. L. Happy and A. Routray, Fuzzy histogram of optical flow orientations for micro-expression recognition, *IEEE Transactions on Affective Computing* **10** (2019) 394, https://doi.org/10.1109/TAFFC.2017.2723386.

22. W. Weng *et al*., Wavelet-based image denoising in (digital) particle image velocimetry, *Signal Processing* **81** (2001) 1503. https://doi.org/10.1016/S0165-1684(01)00047-0.

23. R. J. Adrian and J. Westerweel, Particle image velocimetry, 30 (Cambridge University Press, 2011).

24. W. Hongwei *et al*., The Optical Flow Method Research of Particle Image Velocimetry, *Procedia Engineering* **99** (2015) 918 https://doi.org/10.1016/j.proeng.2014.12.622.

25. A. J. Smits, Flow visualization: techniques and examples (World Scientific, 2012).

26. V. E. Tarasov, Fractional dynamics: applications of fractional calculus to dynamics of particles, fields and media (Springer Science & Business Media, 2011).

27. N. Benkhettou, A. M. B. da Cruz, and D. F. M. Torres, A fractional calculus on arbitrary time scales: fractional differentiation and fractional integration, *Signal Processing* **107** (2015) 230, https://doi.org/10.1016/j.sigpro.2014.05.026.

28. K. Razminia, A. Razminia, and J. J. Trujilo, Analysis of radial composite systems based on fractal theory and fractional calculus, *Signal Processing* **107** (2015) 378. https://doi.org/10.1016/j.sigpro.2014.05.008.

29. H. A. Jalab and R. W. Ibrahim, Fractional Alexander polynomials for image denoising, *Signal Processing* **107** (2015) 340. https://doi.org/10.1016/j.sigpro.2014.06.004.

30. N. Sebaa *et al*., Application of fractional calculus to ultrasonic wave propagation in human cancellous bone, *Signal Processing* **86** (2006) 2668, https://doi.org/10.1016/j.sigpro.2006.02.015.

31. D. Tian, D. Li, and Y. Zhang, Medical image segmentation based on fractional-order derivative, In 2015 Asia-Pacific Energy Equipment Engineering Research Conf. (Atlantis Press, 2015)., https://doi.org/10.2991/ap3er-15.2015.107.

32. J. Zhang and K. Chen, Variational image registration by a total fractional-order variation model, *Journal of Computational Physics* **293** (2015) 442, https://doi.org/10.1016/j.jcp.2015.02.021.

33. Y.-H. Yuan, Q.-S. Sun, and H.-W. Ge, Fractional-order embedding canonical correlation analysis and its applications to multiview dimensionality reduction and recognition, *Pattern Recognition* **47** (2014) 1411, https://doi.org/10.1016/j.patcog.2013.09.009.

34. I. Petrás, Fractional-order nonlinear systems: modeling, analysis and simulation (Springer Science & Business Media, 2011),

35. R. Hilfer (ed.), Applications of Fractional Calculus in Physics (World Scientific, 2000).

36. B. Bonilla, A. A. Kilbas and J. J. Trujillo, Calculo fraccionario y ecuaciones diferenciales fraccionarias (Madrid, UNED, 2003).

37. A. Melbourne *et al*., Using fractional gradient information in non-rigid image registration: application to breast MRI, In Medical Imaging 2012: Image Processing, vol. 8314 (International Society for Optics and Photonics, 2012) p. 83141Z, https://doi.org/10.1117/12.911173.

38. A. Ibeas *et al*., Vaccination controllers for SEIR epidemic models based on fractional order dynamics, *Biomedical Signal Processing and Control* **38** (2017) 136, https://doi.org/10.1016/j.bspc.2017.05.013.

39. M. D. Ortigueira and J. A. T. Machado, Fractional calculus applications in signals and systems, *Signal Processing* **86** (10) (2006) 2503, https://doi.org/10.1016/j.sigpro.2006.02.001.

40. O. Olarte and K. Barbé, Fractional models in electrical impedance spectroscopy data for glucose detection, *Biomedical* Signal Processing and Control **40** (2018) 180, https://doi.org/10.1016/j.bspc.2017.09.017.

41. J. T. Machado, Fractional order describing functions, *Signal Processing* **107** (2015) 389, https://doi.org/10.1016/j.sigpro.2014.05.012.

42. R. Magin *et al*., On the fractional signals and systems, *Signal Processing* **91** (2011) 350, https://doi.org/10.1016/j.sigpro.2010.08.003.

43. J. T. Machado *et al*., Fractional order electromagnetics, *Signal Processing* **86** (2006) 2637, https://doi.org/10.1016/j.sigpro.2006.02.010.

44. J.-B. Li, Gabor filter based optical image recognition using Fractional Power Polynomial model based common discriminant locality preserving projection with kernels, *Optics and Lasers in Engineering* **50** (2012) 1281, https://doi.org/10.1016/j.optlaseng.2012.03.007.

45. X. Chen *et al*., Fractional low-order independent component analysis for face recognition robust to partial occlusion, In Biometrics and Security Technologies (ISBAST), 2014 International Symposium on (IEEE, 2014) pp. 1-5, https://doi.org/10.1109/ISBAST.2014.7013084.

46. N. Paragios, Y. Chen, and O. Faugeras, Handbook of mathematical models in computer vision (Springer, 2010), .

47. E. H. Adelson and J. R. Bergen, Spatiotemporal energy models for the perception of motion, *J. Opt. Soc. Am.* **2** (1985) 284, https://doi.org/10.1364/JOSAA.2.000284.

48. Z. Tu, R. Poppe, and R. C. Veltkamp, Adaptive guided image filter for warping in variational optical flow computation, *Signal Processing* **127** (2016) 253, https://doi.org/10.1016/j.sigpro.2016.02.018.

49. D. Fleet and A. D. Jepson, Computation of component image velocity from local phase information, *Int. J. Comput. Vis.* **5** (1990) 77, https://doi.org/10.1007/BF00056772.

50. D. Fleet and Y. Weiss, Mathematical Models in Computer Vision: The Handbook, chap. *Optical flow estimation*, pp. 239-258 (Springer, 2005),

51. Y. Mochizuki *et al*., Variational method for super-resolution optical flow, *Signal Processing* **91** (2011) 1535, https://doi.org/10.1016/j.sigpro.2010.11.010.

52. J.-d. Kim and J. Kim, Effective nonlinear approach for optical flow estimation, *Signal processing* **81** (2001) 2249, https://doi.org/10.1016/S0165-1684(01)00103-7.

53. D. D. Giusto and G. Vernazza, Optical flow calculation from feature space analysis through an automatic segmentation process, *Signal Processing* **16** (1989) 41, https://doi.org/10.1016/0165-1684(89)90112-6.

54. B. K. P. Horn and E. J. Weldon, Direct methods for recovering motion, *International Journal of Computer Vision* **2** (1988) 51, https://doi.org/10.1007/BF00836281.

55. I. Podlubny, Fractional differential equations: an introduction to fractional derivatives, fractional differential equations, to methods of their solution and some of their applications (Academic press, 1998),

56. B. D. Lucas and T. E. A. Kanade, An iterative image registration technique with an application to stereo vision, *Proceedings of Imaging Understanding Workshop* (1981) 121,

57. B. Horn, Robot vision (MIT Press, 1986).

58. B. Horn, Y. Fang, and I. Masaki, Time to contact relative to a planar surface, *In Proceedings of IEEE conference on Intelligent Vehicles Symposium* (2007) pp. 68-74, https://doi.org/10.1109/IVS.2007.4290093.

59. N. Papenberg *et al*., Highly Accurate Optic Flow Computation with Theoretically Justified Warping, *International Journal of Computer Vision* **67** (2006) 141, https://doi.org/10.1007/s11263-005-3960-y.

60. Z. Tu *et al*., A combined post-filtering method to improve accuracy of variational optical flow estimation, *Pattern Recognition* **47** (2014) 1926, https://doi.org/10.1016/j.patcog.2013.11.026.

61. E. Meinhardt-Llopis and J. Sánchez, Horn-schunck optical flow with a multi-scale strategy, Image Processing on line (2013), .

62. S. Oron, A. Bar-Hille, and S. Avidan, Extended lucas-kanade tracking, In Computer Vision-ECCV 2014: 13th European Conference, Zurich, Switzerland, September 6-12, 2014, Proceedings, Part V 13 (Springer, 2014) pp. 142-156, https://doi.org/10.1007/978-3-319-10602-110.

63. E. Antonakos *et al*., Feature-based lucas-kanade and active appearance models, *IEEE Transactions on Image Processing* **24** (2015) 2617, https://doi.org/10.1109/TIP.2015.2431445.

64. A. Bruhn, J. Weickert, and C. SchnÃ¶rr, Lucas/Kanade meets Horn/Schunck: Combining local and global optic flow methods, International journal of computer vision **61** (2005) 211, https://doi.org/10.1023/B:VISI.0000045324.43199.43.